

The 21 centimeter Background from the Cosmic Dark Ages: Minihalos and the Intergalactic Medium before Reionization

Kyungjin Ahn¹, Paul R. Shapiro¹, Marcelo A. Alvarez¹,
Ilian T. Iliev², Hugo Martel³, and Dongsu Ryu⁴

¹*Department of Astronomy, 1 University Station, C1400, Austin, TX 78712, USA*

²*Canadian Institute for Theoretical Astrophysics, University of Toronto, 60 St. George Street, Toronto, ON M5S 3H8, Canada*

³*Département de physique, de génie physique et d'optique, Université Laval, Québec, QC G1K 7P4, Canada*

⁴*Department of Astronomy and Space Science, Chungnam National University, Daejeon 305-764, Korea*

*E-mail: kjahn@astro.as.utexas.edu, shapiro@astro.as.utexas.edu,
marcelo@astro.as.utexas.edu, iliev@cita.utoronto.ca, hmartel@phy.ulaval.ca,
ryu@canopus.cnu.ac.kr*

Abstract

The H atoms inside minihalos (i.e. halos with virial temperatures $T_{\text{vir}} \leq 10^4\text{K}$, in the mass range roughly from $10^4 M_{\odot}$ to $10^8 M_{\odot}$) during the cosmic dark ages in a ΛCDM universe produce a redshifted background of collisionally-pumped 21-cm line radiation which can be seen in emission relative to the cosmic microwave background (CMB). Previously, we used semi-analytical calculations of the 21-cm signal from individual halos of different mass and redshift and the evolving mass function of minihalos to predict the mean brightness temperature of this 21-cm background and its angular fluctuations. Here we use high-resolution cosmological N-body and hydrodynamic simulations of structure formation at high redshift ($z \gtrsim 8$) to compute the mean brightness temperature of this background from both minihalos and the intergalactic medium (IGM) prior to the onset of Ly α radiative pumping. We find that the 21-cm signal from gas in collapsed, virialized minihalos dominates over that from the diffuse shocked gas in the IGM.

Key words: cosmology, theory, diffuse radiation, intergalactic medium, large-scale structure of universe, radio lines

1 Introduction

Neutral hydrogen atoms in the early universe can be detected in absorption or emission against the cosmic microwave background (CMB) at redshifted radio wavelength 21 cm, depending upon whether their spin temperature T_S is less than or greater than that of the CMB, respectively. Minihalos which form during the “dark ages” have density and temperature high enough to appear in emission (Iliev et al. 2002, 2003). The intergalactic medium (IGM), on the other hand, appears in either emission or absorption. New radio telescopes are being designed to detect this 21 cm signal.

Iliev et al. (2002, ISFM hereafter) showed that atomic collisions inside minihalos are sufficient to decouple the spin temperature of the neutral hydrogen from the CMB temperature. They predicted the mean and angular fluctuations of the corresponding 21cm signal by a semi-analytical calculation based upon integrating the individual minihalo contributions for different halo masses and redshifts, over the evolving statistical distribution of minihalo masses in the Λ CDM universe. The fluctuations, they found, are substantial enough to be detectable with future radio telescopes. Furlanetto & Loeb (2004), on the other hand, have recently suggested that the gas in the diffuse IGM (prior to the onset of Ly α radiative pumping) is also capable of producing the 21cm emission signal and that the IGM contribution to the mean signal will dominate over that from gas inside minihalos.

In order to quantify these effects, we have computed the 21 cm signal both from minihalos and the IGM at $z \gtrsim 8$, using high-resolution cosmological N-body and hydrodynamic simulations of structure formation. We use a flat, Λ CDM cosmology with matter density parameter $\Omega_m = 0.27$, cosmological constant $\Omega_\Lambda = 0.73$, baryon density $\Omega_b = 0.043$, Hubble constant $H = 70 \text{ km s}^{-1} \text{ Mpc}^{-1}$, $\sigma_{8h^{-1}} = 0.9$ and the Harrison-Zel’dovich primordial power spectrum.

2 THE CALCULATION

2.1 Basics of 21 cm Radiation Background from the Dark Ages

Foreground emission or absorption by neutral hydrogen atoms at redshift z is seen against the CMB at redshifted wavelength, $21(1+z)$ cm. The spin temperature (T_S) of a hydrogen atom determines whether the signal is in emission or absorption. Emission occurs when $T_S > T_{\text{CMB}}$, while absorption occurs when $T_S < T_{\text{CMB}}$. T_S can deviate from T_{CMB} in various ways. A hydrogen atom can 1) absorb a 21 cm photon from CMB (CMB pumping), 2) collide with

another atom (collisional pumping) and 3) absorb a Ly α photon to make a Ly α transition, then decay to one of hyperfine 21 cm levels (Ly α pumping).

During the dark ages, when there is no Ly α pumping, the mean 21 cm signal against the CMB will be zero at $z \gtrsim 150$, then in absorption at $20 \lesssim z \lesssim 150$ mostly due to unperturbed IGM, and finally in emission at $z \lesssim 20$ due primarily to minihalos. We restrict ourselves to regions such that the Ly α pumping is negligible even after sources turn on at $z \lesssim 20$. In other words, we only consider collisional pumping in minihalos and the IGM at $8 \lesssim z \lesssim 100$.

2.2 *Semi-analytic calculations*

Here we briefly summarize the semi-analytical calculation of the 21 cm signal from minihalos by ISFM and from the unperturbed IGM. For minihalos, the differential brightness temperature,

$$\delta T_b = \frac{T_S - T_{\text{CMB}}(z)}{1 + z} (1 - e^{-\tau}), \quad (1)$$

is averaged over individual minihalos to give the mean differential antenna temperature $\overline{\delta T_b}$ (for detail, see ISFM). On the other hand, the unperturbed IGM of the universe has a kinetic temperature smaller than the CMB temperature at $z \lesssim 100$, resulting in an absorption signal until collisional pumping becomes negligible at $z \simeq 20$ (Fig. [1]).

2.3 *Numerical Simulations*

We have run a high resolution cosmological N-body and gasdynamic simulation to derive the effects of gravitational collapse and hydrodynamics on the predicted 21 cm signal from the high redshift universe. Our computational box has a comoving size of 0.7 Mpc, with 1024^3 cells and 512^3 dark matter particles, which is optimal for adequately resolving both the minihalos and small-scale structure-formation shocks. We have used the code described in Ryu et al. (1993), which uses the particle-mesh (PM) scheme for calculating the gravity evolution and an Eulerian total variation diminishing (TVD) scheme for hydrodynamics.

In order to calculate the minihalo and the IGM contributions to the total differential brightness temperature, one needs first to identify the halos in the simulation volume. We identified the halos using a friends-of-friends (FOF) algorithm (Davis et al. 1985) with a linking length parameter of $b = 0.25$. The rest of the signal is considered to be from the IGM.

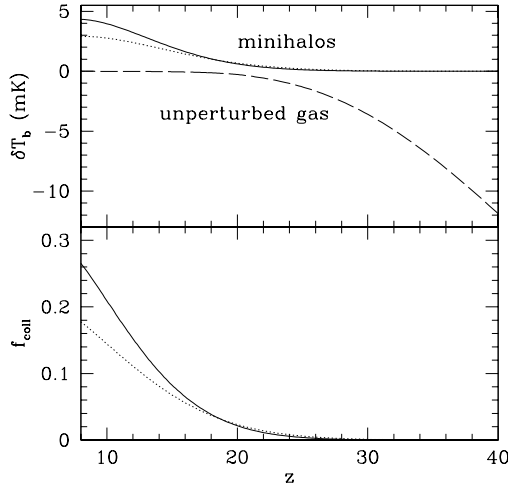


Fig. 1. Analytical prediction for the mean 21 cm differential brightness temperature due to collisionally-decoupled minihalos and an unperturbed IGM. Shown are the results based on the Press-Schechter (solid) and the Sheth-Tormen (dotted) mass functions for halos and the contribution from the IGM gas with cosmic mean density and temperature (dashed). In the bottom panel we show the minihalo collapsed fraction, again based on the Press-Schechter (solid) and the Sheth-Tormen (dotted) mass functions.

In Figure 2, we show projected maps for three different redshifts. Each contribution from minihalos and the IGM is also plotted. It clearly shows that the signal is in absorption due to the IGM at $z \gtrsim 20$, and after crossing the moment when a mixture of emission from minihalos and absorption from the IGM exists ($z \approx 20$), the signal is predominantly in emission both from minihalos and the IGM at $z \lesssim 20$. In Figure 3, we show the total signal as well as minihalos and the IGM contributions.

2.4 Semi-Analytical Calculation of the Halo Contribution

Our numerical simulations have sufficiently high resolution to find all of the minihalos in the computational box, as well as the large-scale structure formation shocks, but not to resolve the internal structure of the minihalos themselves. As ISFM have shown, in order to obtain the correct 21-cm signal from minihalos one needs to do a full radiative transfer calculation through each individual minihalo density profile since, unlike the IGM gas, minihalos have a non-negligible optical depth at the 21-cm line. Hence, we can refine our estimate of the minihalo contribution to the total 21-cm signal by combining our numerical halo catalogues with the semi-analytic calculation of individual minihalo contribution as found by ISFM.

In their approach, the gas density of each minihalo is assumed to follow the

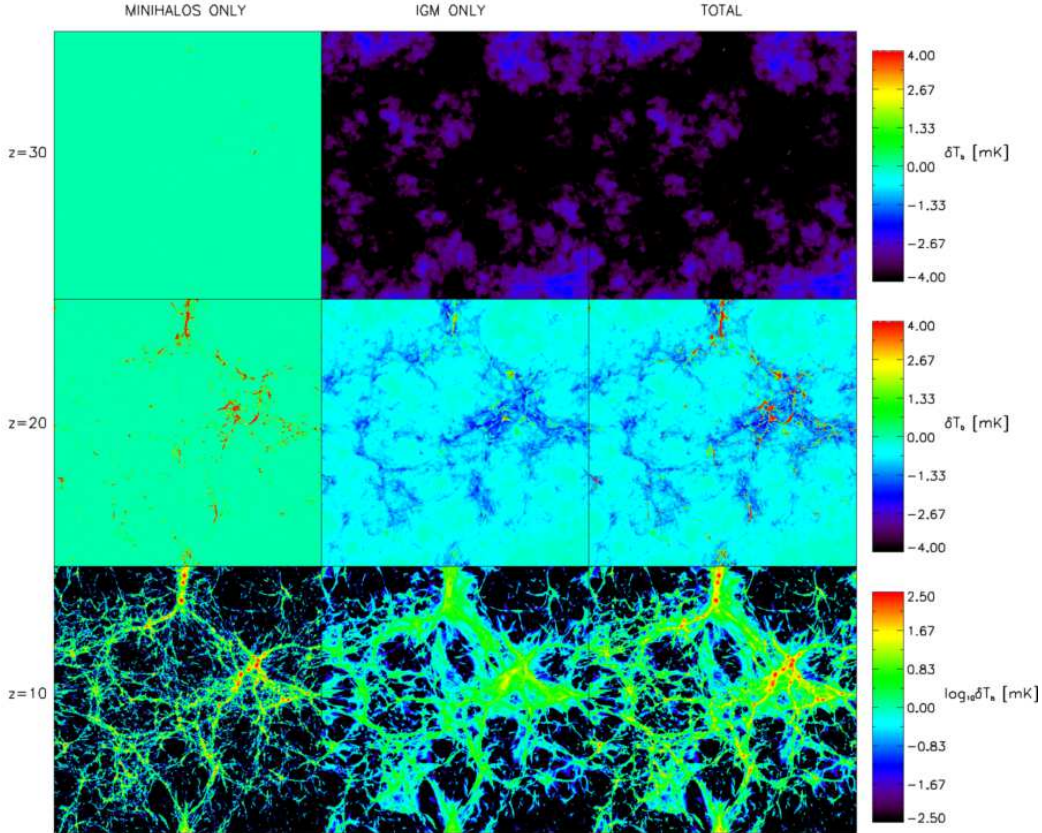


Fig. 2. Map of the 21 cm signal obtained from our high resolution simulation. Rows, top to bottom, show redshifts $z=30$, 20 , and 10 . Columns, left to right, represent contributions from minihalos, the IGM and the total signal, respectively. Note that the scale is linear for the upper two rows of images, but logarithmic for the bottom row.

TIS profile, of Iliev & Shapiro (2001), the radiative transfer calculation is performed for different impact parameters, and then finally the face-averaged δT_b is calculated (see ISFM for details), according to

$$\overline{\delta T_b} = \frac{c(1+z)^4}{\nu_0 H(z)} \int_{M_{\min}}^{M_{\max}} \Delta \nu_{\text{eff}} \delta T_{b, \nu_0} A \frac{dn}{dM} dM. \quad (2)$$

The halo mass function, dn/dM , is provided here, not by the analytical PS mass function as in ISFM, however, but by the halo catalogue we construct from the simulation. Each individual halo contribution, $\Delta \nu_{\text{eff}} \delta T_{b, \nu_0} A$, depends on its mass and redshift of formation (ISFM). Once we calculate $\Delta \nu_{\text{eff}} \delta T_{b, \nu_0} A$, we then obtain the halo contribution using equation (2).

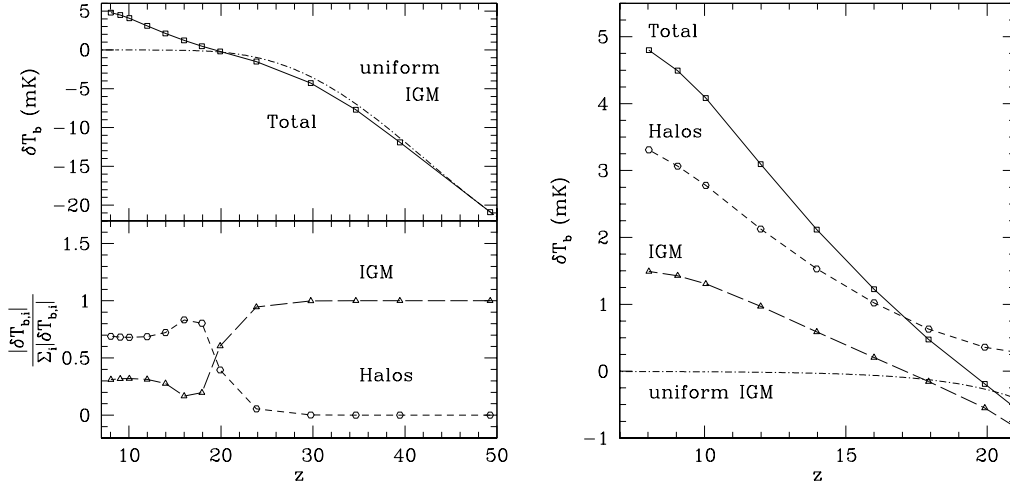


Fig. 3. 21 cm mean brightness temperature evolution. (a)(left) Evolution of the total 21-cm signal vs. redshift. All data points are directly calculated from our simulation box, with the assumption that optical depth is negligible throughout the box. (b)(right) δT_b vs. redshift below $z = 20$. Plotted are the contributions from minihalos (labeled Halos, circles), the IGM (triangles) and the total (squares).

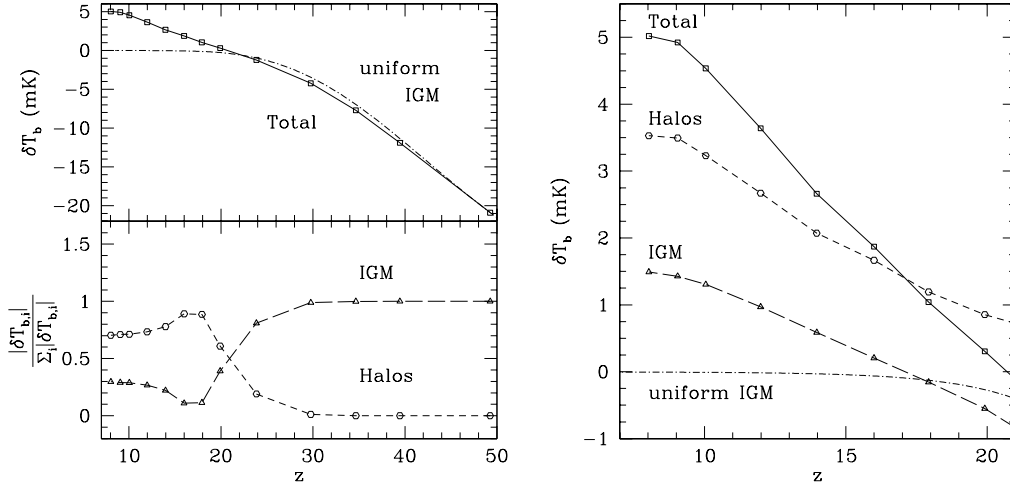


Fig. 4. Semi-analytical minihalo signal vs. IGM signal. The 21 cm flux from each halo in the simulation is found by modeling the halos as described in § 2.4, to estimate the halo 21 cm signal more accurately. Same notation as in Figure 3. The 21 cm minihalo emission increases compared to the raw minihalo signal in figure 3. The IGM signal remains the same.

3 Minihalos vs. the IGM

We find that the emission signal at $z \lesssim 20$ is dominated by minihalos. For $8 \lesssim z \lesssim 14$, about 70 – 80% of the total signal is contributed by minihalos. The minihalo contribution peaks at $z \simeq 16 - 18$, because the IGM is in both

emission and absorption. At $z \simeq 20$, the IGM is mostly in absorption, with an absolute amplitude which is comparable to the minihalo emission signal. Only when the collapsed fraction of baryons into minihalos is negligible ($z \gtrsim 20$), does the IGM make the dominant contribution to the total signal, which is in absorption. Note that the total signal at $z \gtrsim 20$ is slightly stronger than the analytical value for the unperturbed IGM, because clumping of the IGM makes the collisional coupling of the spin temperature to the kinetic temperature slightly stronger.

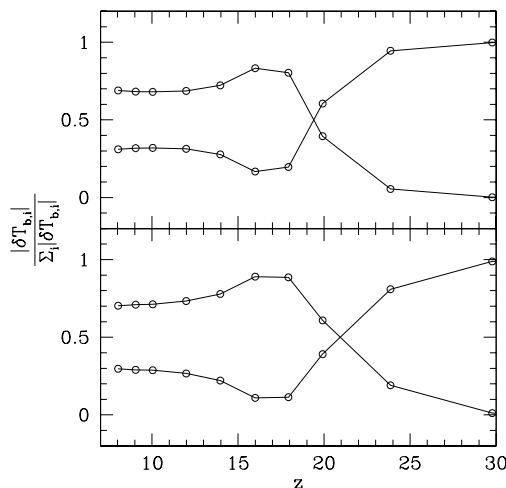


Fig. 5. Fractional contributions of minihalos and diffuse IGM gas to the total 21-cm background. The top panel shows the results obtained directly from simulations (C1: triangle, long-dashed; C2: square, short-dashed; C3: pentagon, dotted; C4: circle, solid). The bottom panel shows the results which were semi-analytically refined (§ 2.4; point- and line-types follow those of the top panel).

4 Conclusions

We have performed a cosmological N-body and hydrodynamic simulation of the evolution of dark matter and baryonic gas in the Λ CDM universe at high redshifts ($8 \lesssim z \lesssim 100$). With the assumption that radiative feedback effects from the first light sources are negligible, we calculated the 21 cm mean differential brightness temperature signal. The mean global signal is in absorption against the CMB above $z \simeq 20$ and in overall emission below $z \simeq 18$. At $z \gtrsim 20$, the density fluctuations of the IGM gas are largely in the linear regime, and their absorption signal is well approximated by the one that results from assuming uniform gas at the mean adiabatically-cooled IGM temperature. At $z \lesssim 20$, nonlinear structures become common, both minihalos and clumpy, warm, mildly nonlinear IGM, resulting in an overall emission at 21 cm with differential brightness temperature of order a few mK.

By identifying the halos in our simulations, we were able to separate and compare the relative contributions of the halos and the IGM gas to the total signal. We find that the emission from minihalos dominates over that from the IGM outside minihalos, for $z \lesssim 20$. The minihalos contribute 70 – 80 % of the total emission signal at $z < 16$, exceeding $\gtrsim 85$ % at $z \simeq 16-18$, and balancing the absorption by the IGM gas at $z \approx 20$. In contrast, the absorption by cold IGM gas dominates the total signal for $z > 20$, with a signal close to that of an unperturbed IGM.

References

- Davis, M., Efstathiou, G., Frenk, C.S. & White, S.D.M., 1985, ApJ, 292, 371
Furlanetto, S.R. & Loeb, A., 2004, ApJ, 611, 642
Iliev, I.T., Scannapieco, E., Martel, H. & Shapiro P.R., 2003, MNRAS, 341, 81
Iliev, I.T. & Shapiro, P.R., 2001, MNRAS, 325, 468
Iliev, I.T., Shapiro, P.R., Ferrara, A. & Martel, H., 2002, ApJ, 572, L123
Ryu, D., Ostriker, J.P., Kang, H. & Cen R., 1993, ApJ, 414, 1